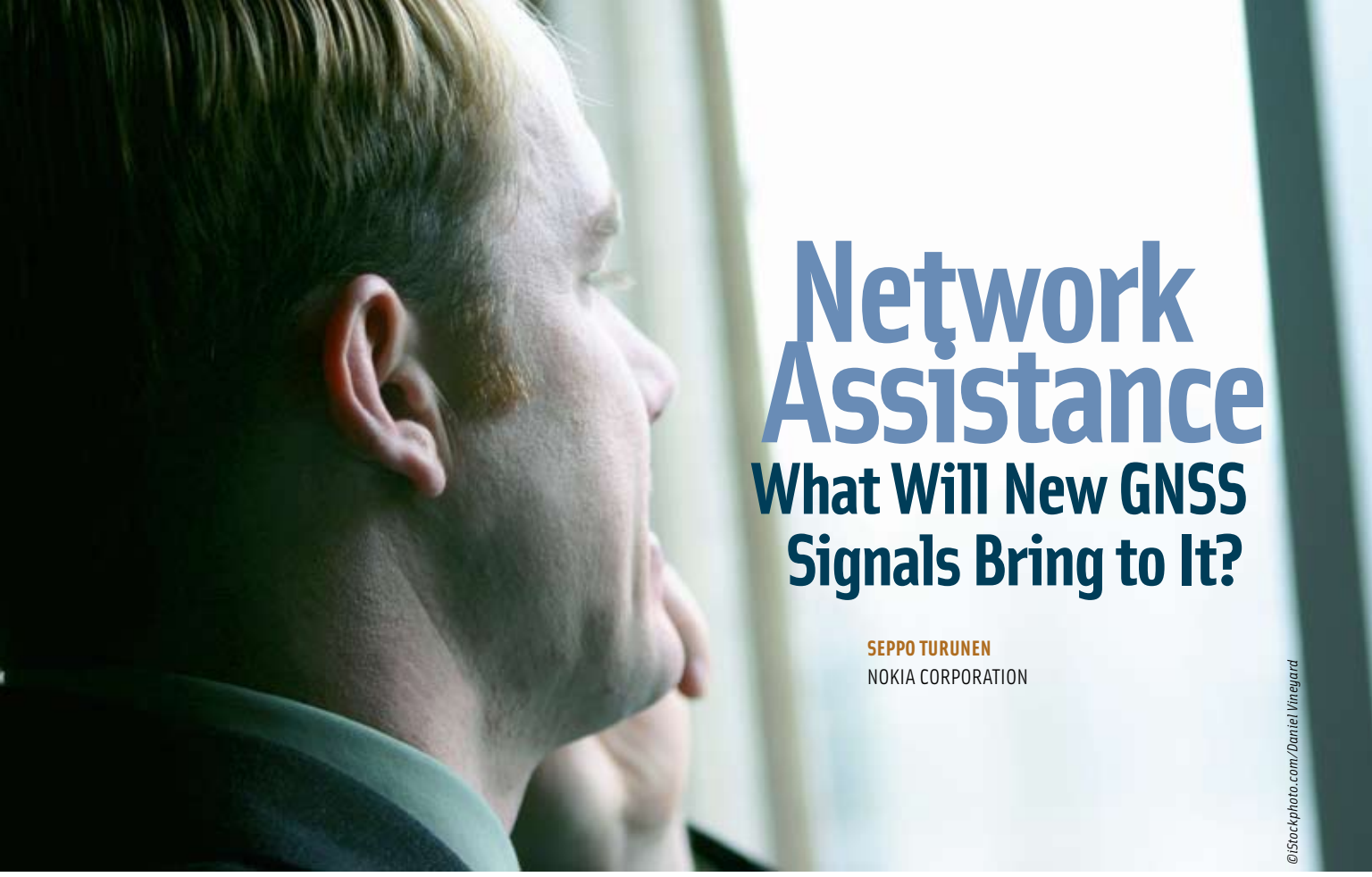

Network Assistance

What Will New GNSS Signals Bring to It?

SEPPO TURUNEN
NOKIA CORPORATION

All GNSS signals are not created equal, and consequently their performance under different kinds of operating environments and using different signal-processing techniques will vary. Rapidly growing GNSS consumer markets are seeing an increase in GNSS receivers that exploit assistance information provided by wireless communications networks to improve performance in challenging environments in cities and indoors. This article by a Nokia senior technologist takes a look at how the many new GNSS signals coming on line might be expected to perform in assisted GNSS and autonomous modes.

Globally GNSS markets are experiencing a sharp growth in sales of consumer products and services. Among these is a cluster of applications known collectively as location based services (LBS), a rapidly evolving field of wireless data services that provide users of mobile terminals with information about their surroundings. As a typical example, travellers can receive directional assistance using downloaded digital maps on which graphical symbols indicate points of interest.

Almost invariably, location based services are delivered using mobile handsets and cellular telephone networks and, ever more often, satellite positioning. Although many LBS applications take place outdoors with unobstructed radiovisibility to GNSS satellites, most will also be used in urban areas and indoors where GNSS signal reception is more problematical. Emergency call positioning is an example of a service that must work both indoors as well as outdoors. However, low-power spread spectrum GNSS satellite signals suffer heavy attenuation in penetrating structures and obstacles.

Due to a strong inverse dependency of dwell time on signal power, traditional sequential-search GNSS receivers have difficulty in acquiring satellite signals if obstructions exist in the signal path. Consequently, assistance techniques that use the wireless communications infrastructure to improve signal acquisition speed and sensitivity are becoming ever more common, and the industry is currently perfecting receiver designs and deploying new network services to exploit these techniques' potential to the full. Moreover, new cellular standards now include stringent sensitivity requirements and test specifications to ensure that the GNSS receivers integrated in mobile phones operate properly under weak signal conditions.

The design of consumer GNSS receivers is still mainly focused on GPS C/A-code reception; however, GNSS providers are envisaging signals with new coding and modulation schemes. These include the new GPS civil signal that transmits on the L2 frequency as well as the new signals that the European Galileo system

now under development will transmit. Because of differences in such variables as frequency allocation, transmission power, and signal structure, these new signals and receiver designs options present a range of possibilities for their practical performance in autonomous and assisted modes.

As is typical of most air interface standards, the related interface control documents (ICDs) focus on the technical specifications of the signals in space and avoid discussing receiver operation and performance. Supplementary analysis is therefore needed in order to set realistic performance targets for future receivers and make informed choices as to which GNSS signals might offer optimal performance.

This article analyzes the expected performance of GPS and Galileo signals in assisted and unassisted modes. It begins with a discussion of state-of-the-art receiver design and signal processing techniques, discusses the assisted GNSS (A-GNSS) mode, and key features of the various GNSS signals.

The article then introduces a numerical scheme for evaluating the theoretical and practical performance of these signals in both assisted and unassisted modes. A key metric introduced in this methodology, attenuation margin, represents the maximum acceptable power loss in a GNSS signal path. The article concludes by assessing the relative performance of GNSS signals in assisted and unassisted mode in terms of the attenuation margin.

GNSS Signal Processing

Typically, GNSS receivers require a reception time of one second or longer in order to detect heavily attenuated GNSS signals, particularly when oscillator instability, signal modulation, or receiver movement preclude the use of long coherent integration times. Under such conditions a serial signal search would proceed extremely slowly, especially when the receiver lacks prior information about code phases or Doppler shifts. As a result, GNSS receivers are ever more often equipped with efficient means of parallel acquisition that allow the processing of the signal search space to be done in a small number of steps or, ideally, in just one step.

A typical parallel acquisition processor consists of a matched filterbank for code phase search and a digital Fourier transformer for frequency domain search. A recent trend is to use software-based acquisition and to perform matched filtering in the frequency domain, which is computationally efficient. The frequency domain processing is typically carried out using data previously sampled into memory, and the required transforms between the time and frequency domains are performed with a fast Fourier transform (FFT).

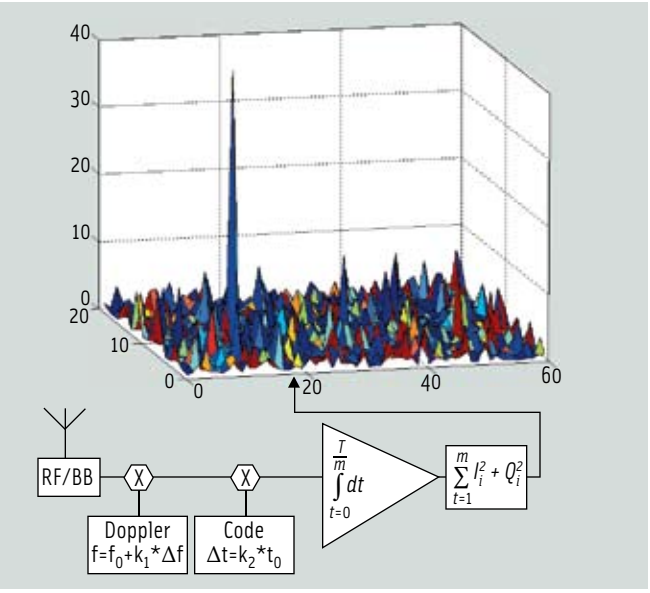

FIGURE 1 Receiver structure for parallel acquisition and signal processing

The processing of one time/frequency bin is shown conceptually in **Figure 1**. A stream of complex baseband samples from the receiver RF section is multiplied with a locally generated replica signal to eliminate Doppler shift and ranging code, leaving a complex DC signal. The signal is then integrated coherently, squared, and added to a memory location dedicated to a specific combination of Doppler shift and code delay.

This sequence of operations, constituting one noncoherent processing step, is performed once or several times for each combination. Finally, some decision strategy is applied to the results to decide whether or not a satellite signal is present and what its parameters are. Any known data modulated on the signal can also be eliminated.

The different eliminations are linear so that their order of execution can be changed without affecting the end result, which can be used to optimize receiver implementation. A wide range of experimental and commercial implementations has been introduced that are functionally equivalent to that shown in Figure 1.

Numerous studies have been published about sequential acquisition strategies that allocate the same processing hardware on different search bins at different instants of time. Sometimes the hardware is allocated repeatedly on the same bin, a procedure called multiple dwelling. Sequential strategies implicitly assume that acquisition performance is limited by receiver processing capacity. The rapid evolution of digital hardware is, however, making this assumption less relevant. In fact, commercial receivers already contain real-time acquisition processors that handle tens of thousands of delay-frequency bins in parallel.

As more processing capacity becomes available, the properties of the satellite signals and the statistics of the parallel acquisition process itself begin to limit receiver performance. This raises the interesting prospect of determining the physical limits of acquisition sensitivity when processing restrictions are left aside entirely. It turns out that the sensitivity then becomes dependent on the dimension of the search space, which, in turn, depends on the ranging code and on the availability of acquisition assistance.

Assisted GNSS. We can reduce the search space and make signal acquisition easier by externally providing direct or

indirect information about code phases, Doppler shifts, and transmitted data bits. When the assistance is indirect, code delays and Doppler shifts are derived from it in the receiver. Indirect assistance typically consists of satellite ephemerides, reference time, reference frequency, and an initial location estimate.

	Data Channel				Pilot Channel		Encoding	Multiplexing
	Code Length	Symbol Length [ms]	Code Rate [kHz]	Data Rate [Hz]	Code Length	Code Rate [kHz]		
GPS L1 C/A	1023	20	-	50	-	-	BPSK(1)	-
GPS L1C	10230	10	1023	50	1800*10230	1023	BOC(1,1)	code+optional phase
GPS L2C	10230	20	511.5	25 or 50	767250	511.5	BPSK(0.5)	code+time
GPS L5	10*10230	10	10230	50	20*10230	10230	BPSK(10)	code+phase
Galileo E1	4092	4	1023	125	25*4092	1023	BOC(1,1)	code
Galileo E5A	20 * 10230	20	10230	25	100 * 10230	10230	Alt-BOC(15,10)	code+phase
Galileo E5B	4 *10230	4	10230	125	100 * 10230	10230	Alt-BOC(15,10)	code+phase
Galileo E6	5115	1	5115	500	100*5115	5115	BPSK(5)	code

TABLE 1. Present and future GNSS signals

AGNSS functionality is included in mobile telephone standards but not yet implemented in all commercial networks. Currently only the GPS L1 C/A signal is covered in the standards but work is going on to extend the coverage to other satellite signals (see the citation, J. Syrjärinne and L. Wirola, referenced in the Additional Resources section at the end of this article).

The reference time and reference frequency could, in principle, be obtained from a local crystal oscillator, but present consumer-grade oscillators are too prone to temperature drift and other instabilities to maintain the required accuracy. Fortunately, cellular base stations have high-quality oscillators and can provide frequency and time references that are accurate enough for Doppler shift estimation. However, the accuracy of absolute time is not always good enough for code phase estimation because the components needed to synchronize the cellular network to the GNSS system time are often missing.

New GNSS Signals

A GNSS signal with ample power and short ranging code can be reliably detected after a reasonably short integration period. Short integration requirements offer the additional benefit of yielding wide frequency-uncertainty bands so that the receiver does not have an excessive number of frequency hypotheses to test. Unfortunately, the planned new GNSS signals have low power and long ranging codes in comparison with the present GPS C/A-code signal and, thus, do not support easy acquisition.

Ranging codes influence signal acquisition mainly through their length, especially if their correlation properties are so good that interference from the signals themselves is insignificant in comparison with the noise component. This influence is twofold. First, a direct linear dependency exists between the search space dimension and the code length. Secondly, the code length may force the receiver to use an otherwise unnecessarily long integration time, thereby narrowing its bandwidth and increasing the number of frequency search bands.

The code length may restrict the choice of integration time if integration over a non-integer multiple of code cycles would undermine the correlation properties of the code. Short codes should present no problem because the integration is, in any case, likely to extend over several code cycles, removing the need to integrate over fractional cycles. Moreover, very long codes may allow termination of the integration phase without needing to complete a full code cycle in order to achieve an acceptable correlation performance.

The original GPS specification dedicated the short C/A code to acquisition and the longer P(Y) code to tracking. No similar distinction is made in the GPS interface specifications for the new L1C [IS-GPS-800], L2C [IS-GPS-200C], and L5 [IS-GPS-705] signals, nor in the Galileo specifications [GAL OS SIS ICD] for the E1, E5, and E6 signals. Instead, all signal components in both systems have relatively long ranging codes, and many of them also have high bit rates. Consequently, their bit energies are lower and search spaces wider than those of the GPS L1 C/A signal and their acquisition, therefore, more difficult.

The new GPS and Galileo specifications introduce pilot signals as a new feature. The specifications do not clearly indicate whether the pilots should be used for tracking, acquisition, or both.

The new signals have long ranging codes, which makes their use for unassisted acquisition more difficult. On the other hand, their lack of data modulation permits coherent integration over multiple bit periods, which yields high processing gain and potentially high receiver sensitivity. However, the actual achievement of higher sensitivity is not immediately evident because the associated search space is large and could give rise to a high false alarm rate that negates the effect of the processing gain.

The dimension of acquisition search space is a product of four factors: length of ranging code, number of frequency search bands, time domain oversampling ratio, and frequency domain oversampling ratio. The number of frequency search bands is proportional to the coherent integration time because the latter is inversely proportional to receiver bandwidth.

The usable coherent integration time of a data signal with unknown content is limited to its symbol length while a pilot signal can, in principle, be integrated indefinitely. In practice, however, coherent integration time is limited to one second or less due to oscillator instability and user movement.

Table 1 shows the code length, symbol length, code rate, and data rate of some freely accessible present and future GNSS signals along with their method of chip encoding and multiplexing. The code lengths of concatenated codes are expressed as the product of the lengths of their constituent codes. Note that the range of code lengths in the table is almost three orders of magnitude.

Noise Bins and Parallel Acquisition

Useful insight into parallel acquisition can be gained by examining the statistics of noise bins in the signal search space. As is well known, the sum of squares of m independent, complex, zero-mean Gaussian random variables of the same variance is non-centrally chi-square distributed with $2m$ degrees of freedom. This is the case with the noise bins when there are m coherent integrations and the receiver input is white noise.

Assume that the noise power and the total reception time are such that the noise variance at both outputs of the complex integrator, when m is taken to be one, is equal to σ^2. In that case, the cumulative distribution function (CDF) of a noise bin, when m is arbitrary, is

$$F(x)=\left(\frac{1}{2\sigma^2}\right)^m \frac{1}{\Gamma(m)}\int_0^{mx} t^{m-1}\exp\left(-\frac{t}{2\sigma^2}\right)dt = \mathrm{P}\left(m,\frac{mx}{2\sigma^2}\right) \quad (1)$$

The expression on the right-hand side is the incomplete Gamma function (discussed in the reference by M. Abramowitz and I. A. Stegun (ed.) cited in Additional Resources), which can be directly evaluated with common numerical software packages. The mean value of the distribution is $2\sigma^2$ which, as could be expected, does not depend on m since it represents the total received energy. The standard deviation (STD), in contrast, depends on m according to the expression $2\sigma^2/\sqrt{m}$.

Parallel acquisition depends on a comparison between the strongest noise bin and the signal bin, and the relevant probability distribution is therefore not that of an individual noise bin but that of the maximum of all noise bins. The CDF of the latter distribution is obtained by raising the CDF of the former distribution to the power of n — n being the total number of noise bins.

Extreme value theory proves that the CDF F_n of the limiting distribution of the maximum of n independent and identically distributed random variables with CDF F, when n tends to infinity, has one of three possible functional forms depending on the tail of the parent distribution F (see the text by E. J. Gumbel in Additional Resources for further discussion of this point). For the chi-square distribution and other distributions with an exponentially decreasing tail, the limiting distribution has the double exponential form

$$F_n(x)=\exp(-\exp(-\alpha_n(x-u_n))), \quad (2)$$

where the coefficients u_n and α_n are defined by the equations

$$F(u_n)=1-\frac{1}{n} \quad (3)$$

and

$$\alpha_n = nF'(u_n) \quad (4)$$

The distribution (2) has the mean value

$$\bar{x}_n = u_n + \frac{\gamma}{\alpha_n} \quad (5)$$

and the standard deviation

$$\sigma(x_n)=\frac{\pi}{\sqrt{6}}\cdot\frac{1}{\alpha_n}, \quad (6)$$

where γ is the Euler constant with the approximate value of 0.5772.

When only one coherent integration step is involved, (1) can be directly substituted into (3) and (4) to yield

$$u_n = 2\sigma^2 \ln(n) \quad (7)$$

and

$$\alpha_n = \frac{1}{2\sigma^2} \quad (8)$$

Using these values in (5) and (6) gives

$$\bar{x}_n = 2\sigma^2(\ln(n)+\gamma) \quad (9)$$

and

$$\sigma(x_n)=\pi\sqrt{\frac{2}{3}}\sigma^2 \quad (10)$$

From (9) and (10), then, we can see that the expected value of the maximum of the chi-square distributed noise bins depends logarithmically on n, while the standard deviation of the maximum is constant. Broadly speaking, the graph of the probability density function (PDF) of the noise maximum retains its shape but shifts horizontally when the size of the search space is changed. This means that signal detection thresholds have to be shifted accordingly in order for error probabilities to remain constant, and a larger search space thus implies lower acquisition sensitivity.

In particular, when there is only one coherent integration step, the signal power required to maintain a constant failure rate is inversely proportional to the logarithm of the search space dimension. In an earlier article in *Coordinates* magazine, January 2007, the author discussed the case in which m is a small integer different from unity and showed that the mean value of the distribution (2) then also has an essentially logarithmic dependency on n and a nearly constant standard deviation.

Borio et al (see Additional Resources) propose the use of so-called system probabilities to characterize parallel acquisition receivers. *System false alarm probability in the absence of signal* is defined as the probability of at least one noise bin in a search space of dimension n exceeding a given detection threshold q. It can be expressed in terms of the false alarm probability P_{fa} of a single time/frequency search cell as

Signal	Nominal Power [dBm]	Coherent Integrations	Unassisted Acquisition Δ f = 10 kHz				Assisted Acquisition Δ f = 100 Hz, Δ t = 10 υs				Single Cell Detection	
			Delay Bins	Frequency Bins	E/2σ2 [dB] P_{FA}=0.01 P_D=0.99	Attenuation Margin [dB]	Delay Bins	Fre-quency Bins	E/2σ2 [dB] P_{FA}=0.01 P_D=0.99	Attenuation Margin [dB]	E/2σ2 [dB] P_{fa}=0.01 P_d=0.99	Attenuation Margin [dB]
GPS L1 C/A	-128.50	50	1 023	300	19.06	22.40	10	3	17.45	24.05	16.39	25.10
GPS L1C Data	-133.00	100	20 460	150	20.40	16.60	20	2	18.69	18.31	17.60	19.40
GPS L1C Pilot	-128.25	1	36 828 000	15 000	17.25	23.94	20	150	14.29	26.90	11.49	39.70
GPS L2C Data	-133.00	50	20 460	300	19.42	17.58	5	3	17.45	19.55	16.39	20.61
GPS L2C Pilot	-133.00	1	1 534 500	15 000	16.87	20.13	5	150	14.15	22.85	11.49	25.51
GPS L5 Data	-127.90	100	102 300	150	20.57	21.53	100	2	19.03	23.07	17.60	24.50
GPS L5 Pilot	-127.90	1	204 600	15 000	16.64	25.46	100	150	14.68	27.42	11.49	30.61
Galileo E1 Data	-130.00	250	8 184	60	21.77	17.82	20	1	20.16	19.43	19.27	20.32
Galileo E1 Pilot	-130.00	1	204 600	15 000	16.65	22.94	100	150	14.29	25.29	11.49	28.10
Galileo E5A Data	-128.69	50	204 600	300	19.65	21.66	100	3	17.98	23.33	16.39	24.92
Galileo E5A Pilot	-128.69	1	1 023 000	15 000	16.84	24.47	100	150	14.68	26.64	11.49	29.83
Galileo E5B Data	-128.69	250	40 920	60	21.95	19.36	100	1	20.51	20.80	19.27	22.05
Galileo E5B Pilot	-128.69	1	1 023 000	15 000	16.84	24.47	100	150	14.68	26.64	11.49	29.83
Galileo E6 Data	-128.00	1000	5 115	15	24.18	17.82	50	1	23.06	18.94	22.00	20.00
Galileo E6 Pilot	-128.00	1	511 500	15 000	16.77	25.23	50	150	14.47	27.53	11.49	30.51

TABLE 2. Parameters and results of numerical examples

$$P_{FA}^{a}(q) = 1 - \left[1 - P_{fa}(q)\right]^{n} \quad (11)$$

or in terms of the noise bin CDF F as

$$P_{FA}^{a}(q) = 1 - \left[F(q)\right]^{n} \quad (12)$$

System detection probability, which takes into consideration multiple search bins, is defined as the probability of the signal bin value exceeding both q and all noise bin values. It can be expressed as

$$P_D(q) = \int_{q}^{\infty} \left[1 - P_{fa}(x)\right]^{n-1} f_A(x)\,dx, \quad (13)$$

where $f_A(x)$ is the PDF of the signal bin. In the case of complex Gaussian noise and m coherent integrations the signal bin follows the non-central chi-square distribution and has the PDF

$$f_A(x) = \frac{m}{2\sigma^2}\left(\frac{mx}{E}\right)^{\frac{m-1}{2}} e^{-\frac{E+mx}{2\sigma^2}} I_{m-1}\left(\frac{\sqrt{mxE}}{\sigma^2}\right) \quad (14)$$

where σ is the noise STD defined earlier, $I_k(x)$ is the modified Bessel function of the first kind of order k, and E is the squarer output in the absence of noise when m is taken to be one. This point is discussed further in the ION article by this author cited in Additional Resources.

Substituting (1) and (14) into (13) and changing the integration variable to $u = mx/\sigma^2$ gives the system detection probability

$$P_D(q) = \frac{1}{2}\int_{\frac{mq}{\sigma^2}}^{\infty} \left(\frac{u}{E/\sigma^2}\right)^{\frac{m-1}{2}} e^{-\frac{E/\sigma^2+u}{2}} I_{m-1}\left(\sqrt{\frac{uE}{\sigma^2}}\right) P\left(m, \frac{u}{2}\right)^{n-1} du \quad (15)$$

When the total reception time T is one second, it follows from the identity

$$E/(2\sigma^2) = PT/(F_N N_0)\,, \quad (16)$$

where F_N is the receiver noise factor, that $E/(\sigma^2)$ in (15) can be interpreted as twice the ratio of signal power P to noise spectral density at receiver baseband input, a quantity customarily measured on a dB-Hz scale.

GNSS Signal Performance

The system detection probabilities for the satellite signals of Table 1 are plotted against the normalized signal energy $E/(2\sigma^2)$ in **Figure 2** (no acquisition assistance) and **Figure 3** (assisted acquisition). The detection threshold q is chosen so that the system false alarm probability as evaluated from (12) and (1) is one percent. The total reception time is taken to be one second.

No acquisition assistance is assumed in Figure 2 so that the search space consists of all code phases and a full frequency uncertainty range, which is taken to be 10 kHz. Acquisition assistance with a time uncertainty of 10 microseconds and a frequency uncertainty of 100 Hz is assumed to be available in Figure 3.

For comparison, the single-cell detection probability P_d is plotted in **Figure 4** using equations (1), (12) and (15) and setting $n = 1$ and $P_{fa} = 0.01$. The numerical evaluation of the equations was done using Matlab standard functions with the exception that the Bessel function, which obtains very large values, was approximated in logarithmic form using a power series described in the previously referenced Abramowitz handbook.

Table 2 gives the receive parameters for Figures 2 and 3. The receiver is assumed to be capable of a one-second coher-

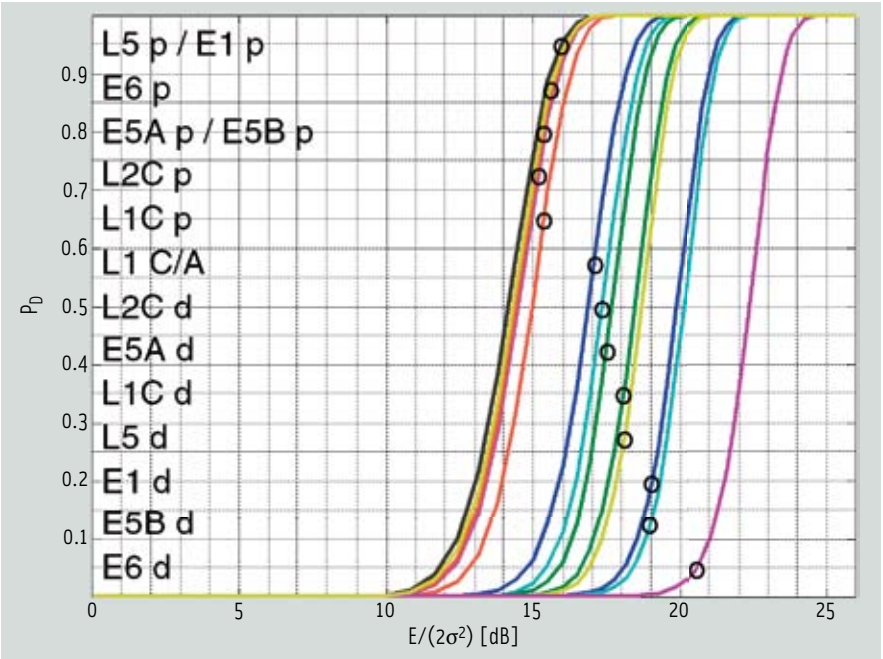

FIGURE 2 System detection probability as a function of normalized signal energy $E/(2\sigma^2)$ in unassisted acquisition (P_{FA} = 0.01)

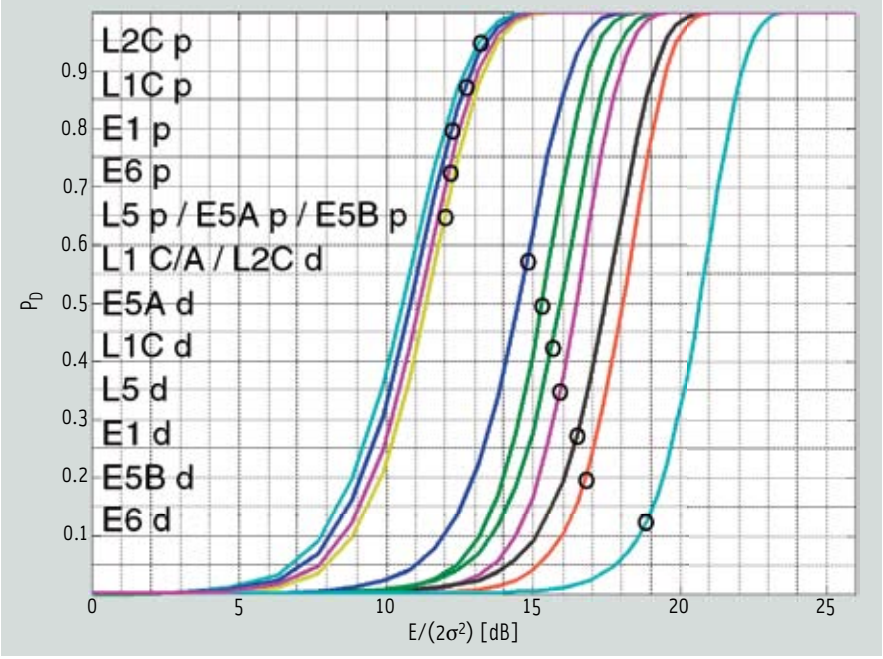

FIGURE 3 System detection probability as a function of normalized signal energy $E/(2\sigma^2)$ in assisted acquisition (P_{FA} = 0.01)

ent integration so that the pilot signals can be processed in a single integration step. The coherent integration time for the data signals is taken to be one bit period. For the BPSK and AltBOC(15,10) modulated signals, one delay bin is assigned for each code element while for the BOC(1,1) modulated signals two bins are assigned.

The number of frequency search bands is calculated from the formula

$$N_f = 1.5 \times BT/m, \quad (17)$$

where B is the frequency uncertainty range. The formula assumes that the width of a frequency search band is two thirds of the inverse coherent integration time. The total number n of search bins is obtained by multiplying the number of delay bins with the number of frequency search bands. Note that the value of n is high, on the order of 10^9, for the unassisted acquisition of pilot signals, but only 15,000 or below when assistance is available.

Table 2 lists the values of $E/(2\sigma^2)$ required to achieve a system detection probability of 0.99 (P_D = 0.99). The table also gives the attenuation margin between the nominal satellite signal power and the required signal power as calculated from (16) when the total implementation loss is 4 dB. The loss is assumed to cover receiver front-end noise, digital processing noise, losses from off-peak sampling, and losses from integrating across bit boundaries.

The nominal satellite signal powers are as specified in the respective ICDs and divided between pilot and data signals as implied by the documents. To account for the constant envelope corrections of the AltBOC(10,15) modulation scheme, 0.69 dB is subtracted from the total power of the Galileo E5 signal.

The L1C pilot signal is assumed to have a high frequency time-multiplexed BOC (TMBOC) signal component that is filtered away, leading to a reduction of power by 4/33. The Galileo E1 data and pilot signals are assumed to have a composite BOC (CBOC) signal component that is likewise filtered away, leading to a reduction of power by 1/11.

The plots show that the unassisted receiver of Figure 2 is significantly less sensitive than the hypothetical single-cell receiver of Figure 4, which is obviously due to the larger search space of the former. For P_D = 0.99 the difference, averaged over all satellite signals, is 4 dB.

The difference in attenuation margins becomes higher the smaller the number of coherent integrations is, as can be seen by comparing the $E/(2\sigma^2)$ values given in Table 2. This can be understood by remembering that a smaller number of coherent integrations results in a larger number of frequency uncertainty bands and, therefore, in a larger search space.

Comparison of Figures 2 and 3 shows that the assisted receiver is more sensitive than the unassisted one. For P_D

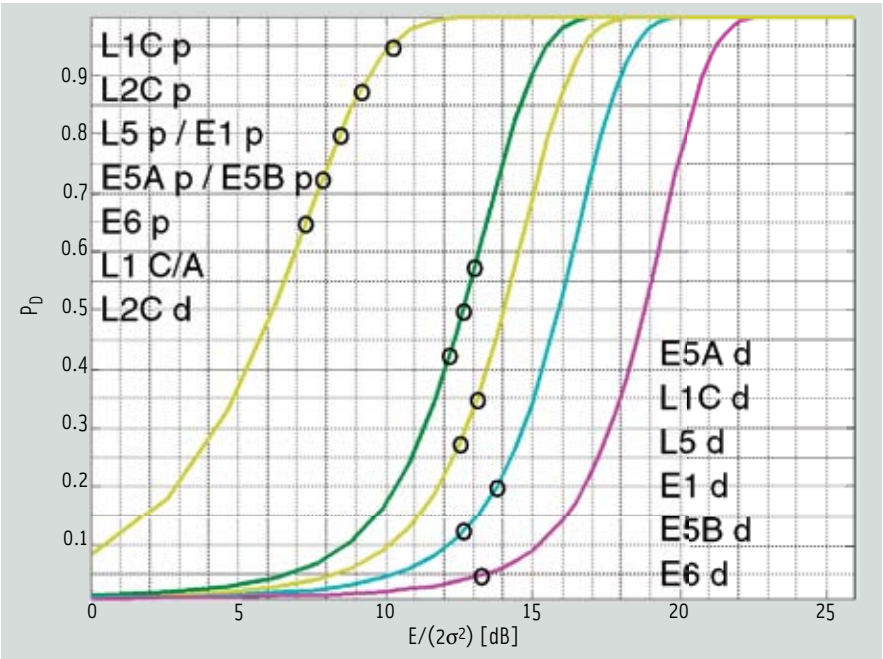

FIGURE 4 Possibility of detection as a function of normalized signal energy $E/(2\sigma^2)$ in single cell acquisition (P_{fa} = 0.01)

= 0.99 the difference, averaged over all satellite signals, is 2 dB. For individual satellite signals the difference can be found by comparing the $E/(2\sigma^2)$ values in Table 2.

The attenuation margins given in Table 2 represent the maximum acceptable loss in signal path. The table reveals that the GPS L1 C/A signal, despite having higher power, has a lower margin than most of the pilot signals. The reason is obviously the shorter coherent integration time of the L1 C/A signal.

The differences between the pilot signals are fairly small and mainly due to different transmission powers. For example, the GPS L5 pilot has a 1.5 dB higher attenuation margin in unassisted mode than the GPS L1C pilot, which is hardly a sufficient reason to convert a receiver to a new band. As can be seen from the table, however, there is the additional motivation that the size of the search space of the L5 receiver is less than one hundredth of that of the L1C receiver.

Conclusion

This article highlights the importance of GNSS acquisition sensitivity for location based services in view of regulations and user expectations. Parallel receiver architectures and terrestrially available assistance were mentioned as means of improving acquisition performance. Extreme value theory was used to gain an insight into the distribution of signals in large search spaces typical of parallel acquisition receivers. The discussion showed that acquisition sensitivity depends approximately on the inverse of the logarithm of the search space dimension.

An analytic expression was derived for system detection probability and used to assess receiver performance in the assisted and unassisted acquisition of several GPS and Galileo signals. The results indicate that while the achievable acquisition sensitivity depends mainly on the length of coherent integration, it is also negatively influenced by the dimension of the search space. The average sensitivity loss attributable to the dimension was 4 dB in unassisted acquisition and 2 dB in assisted acquisition so that an average sensitivity improvement of 2 dB can be attributed to the assistance.

Pilot signals could be acquired at a level 5 dB lower than the corresponding data signals both in the assisted and unassisted cases. However, use of pilots is only practical when assistance is available due to the otherwise extremely high volume of the search space. Taking into consideration the 2 dB improvement from reduction in search space, a total average sensitivity improvement of 7 dB could therefore be achieved by using assistance in the acquisition of the new GNSS signals.

Additional Resources

Abramowitz, M., and I.A. Stegun (ed.), "Handbook of mathematical functions," Dover Publications, 1970.

Borio, D., and L. Camoriano and L. Lo Presti, "Impact of the Acquisition Searching Strategy on the Detection and False Alarm Probabilities in a CDMA Receiver," IEEE/ION PLANS 2006, April 25-27, 2006, San Diego, California.

GAL OS SIS ICD/D.0, Galileo Open Service Signal In Space Control Document, Draft 0, ESA/GJU, May 5, 2006.

Gumbel, E. J., *Statistics of Extremes,* Dover publications, 2004.

IS-GPS-200D, Navstar GPS Space Segment/Navigation User Interfaces, March 7, 2006.

IS-GPS-705, Navstar GPS Space Segment/User Segment L5 Interfaces, January 5, 2005.

IS-GPS-800, Navstar GPS Space Segment/User Segment L1C Interfaces, April 19, 2006.

Kaplan, E.D., and C.J. Hegarty, (ed.) *Understanding GPS Principles and Applications,* Artech House, 2006.

Syrjärinne, J., and L. Wirola, "Setting a New Standard – Assisting GNSS Receivers That Use Wireless Networks," *Inside GNSS*, Vol. 1, Number 7, October 2006.

Turunen, S., "Combinatorial loss in satellite acquisition," ION GNSS 2005, Long Beach, CA, USA, September 13-16, 2005.

Turunen, S., "Acquisition sensitivity limits of new civil GNSS signals," *Coordinates* (cGIT, Delhi, India), Volume III, Issue 1, January 2007.

Author

Seppo Turunen is a principal technologist at Nokia Technology Platforms. He received his M.Sc. in electrical engineering from Tampere University of Technology in Finland. From 1979 to 1988 he was involved in the research and development of industrial process control systems at Valmet Process Automation. He joined Nokia in 1988 and has held several positions at Nokia Research Center, Nokia Mobile Phones, and Nokia Technology Platforms. His current interests include mobile phone positioning techniques based on assisted GNSS, cellular network measurements, and motion sensors.